AAEC/E138

AAEC/E138

AUSTRALIAN ATOMIC ENERGY COMMISSION
RESEARCH ESTABLISHMENT
LUCAS HEIGHTS

SINTERABILITY STUDIES ON VARIOUS BeO POWDERS
A SECOND REPORT

by

M. J. BANNISTER

Issued Sydney, June 1965

UNCLASSIFIED

AUSTRALIAN ATOMIC ENERGY COMMISSION

RESEARCH ESTABLISHMENT

LUCAS HEIGHTS

SINTERABILITY STUDIES ON VARIOUS BeO POWDERS

A SECOND REPORT

by

M.J. BANNISTER

ABSTRACT

Six sulphate-derived beryllium oxide powders have been studied and a comparison made of their powder properties and sintering behaviour. Powders containing segregated impurities showed irregular grain growth and those with strongly bonded aggregates showed internal cracking during sintering. All powders sintered less readily in hydrogen than in nitrogen. Semi-empirical equations are presented relating sintering temperature and the grain size at any sintered density to the powder surface area and the green density of the pressed compact.

CONTENTS

(Continued)

CONTENTS (Continued)

1. INTRODUCTION

This report is the second from a programme to determine factors which are important in the sintering of beryllium oxide. In previous work (Bannister 1964a), a sulphate–derived powder (Brush UOX lot 200–W–216–P) was found to be more sinterable than powders produced by alternative routes. The differences between powders were attributed in part to the varying effects of anions which remained from the different methods of preparation.

The powders discussed in the present report were all sulphate–derived and were similar in cationic impurity content, but they differed in physical properties. Sinterability was found to be related to surface area, green density, and uniformity of crystallite size in the original powder. Crystallite size, green density, the aggregate structure in the powder, and the presence of segregated impurities affected the microstructure developed on sintering.

2, EXPERIMENTAL

2.1 Materials

The powders used are listed in Table 1. Table 2 gives the analysis of each powder.

2.2 Experiments Performed

As in the previous work (Bannister 1964a) the powders were subjected to the following physical tests before assessment of their sinterability.

(a) Examination by transmission optical and electron microscopy.

(b) Surface area measurement (BET method, nitrogen adsorption).

(c) The determination of pour (or bulk) density and of tap density.

The techniques used for pressing of pellets, measurement of green densities, sintering, and the determination of the density and open porosity of each sintered specimen were basically the same as those used before (Bannister 1964a). Powders 5 and 6 were so sinterable that experiments were performed at temperatures down to 1200 °C, whereas the minimum sintering temperature for each of the other powders was 1500 °C.

In the previous work some powders of poor sinterability were found to lower the sintered density of UOX lot 200–W–216–P when specimens of both powders were present in the furnace. No similar effect was shown by any of the powders tested in the present work.

Transverse sections of sintered specimens with densities greater than 95 per cent. theoretical were polished, etched, and examined under the optical microscope. Grain sizes were determined by the mean linear intercept technique (Bannister 1964b). The statistical accuracy of each mean linear intercept quoted was ± (10 to 20) per cent.

3. RESULTS

3.1 Powder Properties

Table 3 contains the measured surface areas, pour and tap densities, green densities after pressing at 20 tons/in^2, and a mean crystallite diameter for each powder calculated from the surface area, assuming spherical crystallites. Also included in Table 3 is the mean linear grain–boundary intercept in each green compact, calculated from the powder surface area using the theory of Smith and Guttman (1953) (see Appendix 1). Of particular interest are the high pour and tap densities, and thus good die–fill properties, of powders 4, 5, and 6.

3.2 Microscopy

Powders 1, 2, and 3 contained loose aggregates of submicron crystallites (Figures 1 to 3).

Powder 1 also contained many needles (perhaps 1 volume per cent.) up to 200 microns long by 40 microns wide, whereas powders 2 and 3 appeared to be free of needles. However powder 3 contained a very wide spread of crystallite sizes (Figure 3) compared with the more uniform powders 1 and 2. Powders 4, 5, and 6 contained dense, hard aggregates from <1 to >100 microns in size, all composed of submicron crystallites. The crystallite sizes of powders 5 and 6 were quite uniform (Figures 5 and 6) whereas powder 4, like powder 3, contained a very wide spread of crystallite sizes (Figure 4).

3.3 Sintering

The densities obtained after sintering compacts of the powders in flowing nitrogen, and in flowing hydrogen, are given in Tables 4 and 5 respectively. In every case the density quoted is the arithmetic mean of duplicate results, which agreed to within 0.02 g/cm^3.

3.4 Open Porosities

The relationships found between open porosity (as measured by water absorption) and total porosity are shown in Figure 7. The solid line is the relationship previously found for UOX lot 200-W-216-P (Bannister 1964b). Only powder 3 showed significantly early pore closure, and no powder showed delayed pore closure relative to previous results. Optical microscopy indicated that the low apparent open porosity of powder 3 specimens was not due to the development of an impermeable skin.

3.5 Metallography

Average grain sizes of specimens sintered in nitrogen, and in hydrogen, are given in Table 6.

Powders 1, 2, and 3 showed similar sintered microstructures, except that powder 1 contained large needles (Figure 8) which were not observed in sintered specimens of powders 2 and 3. All three microstructures showed isolated coarse-grained areas (Figure 9) often with central voids; these areas are atributed to the presence of segregated impurities (such as firebrick) in the original powders. Microprobe analysis (Van Peer and Bannister, unpublished work) has revealed unusually high concentrations of silicon, aluminium, and magnesium in similar areas in sintered specimens from UOX lot-200-W-216-P.

The microstructures of powders 4, 5, and 6 also showed isolated coarse-grained areas, together with occasional areas of very fine grain size. There were no needles present. However the dominant feature of the microstructures produced by these powders was the presence of internal voids or cracks. These were more prevalent at low sintering temperatures where it was apparent that the cracks occurred around small, dense areas in a more porous matrix (Figure 10).

4. DISCUSSION

4.1 Microstructures

Three types of microstructural defect were found in sintered BeO specimens:

(a) Needles – in powder 1 only.

(b) Coarse-grained areas – in all powders.

(c) Internal cracking and density variations – in powders 4, 5, and 6.

The needles found in sintered specimens of powder 1 were present in the original powder (Section 3.2) and also occur in other batches of UOX-grade beryllium oxide, for example lot 200-W-216-P and lot 200-W-269-P. They are probably formed during calcination of the parent beryllium sulphate.

Since sulphate-derived materials from other sources (Table 1) do not contain needles, their formation is probably related to the particular equipment and/or calcination procedure used by the supplier. Needles are coarse grains in what may otherwise be fine-grained BeO and thus may adversely affect those properties, such as modulus of rupture and irradiation resistance, which appear to vary inversely as the grain size.

As stated in Section 3.5, the coarse-grained areas found in sintered specimens of all powders were probably caused by segregated impurities. Some of these may have been introduced into the powders during powder-handling operations prior to pressing, but it is more likely that the impurities were already present in the powders as received. These coarse-grained areas are probable sources of weakness in the BeO, for the following reasons:

(a) Coarse-grained material may be inherently weaker than fine-grained material.

(b) These areas often contain large central voids.

(c) Internal stresses may be set up due to different sintering rates in the coarse-grained areas and the surrounding matrix.

The internal cracks in specimens of powders 4, 5, and 6 sintered at moderate temperatures were located around the edges of circular areas which were denser than the surrounding matrix (Figure 10), but were not of detectably higher impurity content. This density variation disappeared at higher sintering temperatures and the cracks also then tended to heal or round off to elongated voids. The cracking is attributed to stresses developed during sintering between the faster-sintering circular (or spherical, in three dimensions) areas and the slower-sintering matrix. These fast-sintering "spheres" were about the same size as the dense hard aggregates found in the original powders; it is inferred that preferred shrinkage of these aggregates led to the internal cracking and variations in density found after sintering compacts of powders 4, 5, and 6. The cracks shown in Figure 10 would certainly weaken the BeO body. The incidence of cracking might be reduced, without markedly decreasing the sinterability, by grinding the powder to break up aggregates. It is not known why these aggregates occur in the three powders, but it is significant that all three were obtained from the one supplier.

4.2 Effects of Sintering Atmosphere

Tables 4 and 5 confirm the result already reported (Bannister 1964a) that powders containing residual sulphate sinter to slightly lower densities in slowly-flowing hydrogen than in nitrogen. The reduced sinterability in hydrogen could be due to water vapour formed by the reaction:

$$SO_4^{2-} + 4H_2 \longrightarrow O^{2-} + H_2S + 3H_2O \quad , \qquad \ldots\ldots\ldots\ldots (1)$$

Hydrogen sulphide was detected in the furnace outlet gases at quite low temperatures and was apparently eliminated from the furnace atmosphere, under the experimental conditions, below about 700°C. If the water vapour was flushed from the furnace concurrently with H_2S, the mechanism which led to a reduced sintered density must have occurred below 700°C. This temperature seems too low for significant pore-rounding by a vapourization-condensation reaction, the explanation usually offered for the effect of water vapour on the sintering of BeO (Aitken 1960). This may indicate the need for an alternative explanation, such as a water vapour - enhanced surface diffusion process, or the premature removal of sulphate by reaction (1).

No such reaction occurs with dry nitrogen and it is assumed that with this gas "normal" sintering occurs. Nitrogen sintering is discussed more fully in Section 4.4.

4.3 Density-Grain Size Relationships

It was previously shown (Bannister 1964b) that, for vacuum sintering of UOX lot 200-W-216-P of green density 1.73 g/cm^3, the relationship between grain size and density in the range 95-99 per cent. theoretical could be described by the equation:

$$(\text{Porosity})^{1.13} \ (\text{grain size}) = C \quad , \qquad \ldots\ldots\ldots\ldots (2)$$

where C is a constant independent of both sintering temperature and time.

Further work (Bannister, unpublished) has shown that the equation:

$$(\text{Porosity})^{1.25}\ (\text{grain size}) = C' \quad , \qquad \ldots\ldots\ldots\ldots (3)$$

(where C' is also independent of both temperature and time)

applies over a wider range of conditions (for example, UOX lot 200–W–216–P pressed to 1.5 g/cm^3 and sintered at 1600–1700°C, and UOX lot 200–W–266–P pressed to 1.76 g/cm^3 and sintered at 1400–1700°C) and that it can also describe the earlier results equally as well as Equation 2.

The value of the constant C' in Equation 3 was different for each lot of UOX powder, and also varied with green density for UOX lot 200–W–216–P. However substitution in Equation 3 of the relevant green porosity gave a calculated grain size which was close to the mean crystallite diameter of the powder in each case. This result suggested that the equation might be valid even at densities close to the green density and, conversely, that it might be used to predict, from the green porosity and crystallite size of a given powder, the relationship between sintered porosity and grain size.

In the previous work the calculated "grain size" at the green density was smaller than the mean crystallite diameter of each powder. However, as will be shown, this discrepancy occurred because the mean linear intercept rather than the mean grain diameter was taken as a measure of the sintered grain size. To be consistent, either the calculated original grain size should be compared with the mean linear intercept in the powder compact, or alternatively the mean linear intercepts in sintered specimens should be converted to mean grain diameters. The first procedure has been preferred, since the mean linear intercept is the quantity which is measured in intercept grain counting, and is directly related to the measurable property of crystallite surface area per unit volume (Appendix 1); on the other hand, calculation of mean grain diameter involves the assumption of a definite grain shape. Use of the mean linear intercept in each powder compact rather than the mean crystallite diameter gave better agreement with the original grain size calculated from Equation 3. This evidence suggests that Equation 3 can be written as :

$$P^{1.25}G = C' = P_o^{1.25}G_o \quad , \qquad \ldots\ldots\ldots\ldots\ldots (4)$$

where P is the sintered porosity,
P_o is the green porosity,
G is the sintered mean linear intercept, and
G_o is the green mean linear intercept.

The grain size and density data contained in Tables 4, 5, and 6 were used to test whether Equation 4 applied to all the powders examined in the present work; reults are given in Table 7. The possible errors in reported mean linear intercepts were predominantly statistical, and the 99 per cent. confidence limits varied from ±10 to ±20 per cent. of the mean values. The wider confidence limits generally corresponded to the lower grain sizes and thus (see below) to the higher and more accurate porosity values. The errors in porosity measurement were largely experimental, and increased from ±7 per cent. to ±25 per cent. of the reported value, as the porosity changed from 5 to 1.3 per cent. (the lowest experimental porosity). In general, then, the likely accuracy of $(P^{1.25}G)$ was about ±30 per cent., and agreement within these limits with $(P_o^{1.25}G_o)$ is considered satisfactory.

Powders 1 and 2 gave good agreement with Equation 4, except for powder 1 sintered at 1600°C in hydrogen. Powders 5 and 6 satisfied Equation 4 up to 1400°C, and then gave increasingly high results because they reached maximum density at 1400°C (Tables 4 and 5). Powders 3 and 4 did not obey Equation 4, but gave consistently high results. These high values were probably caused by the many large crystallites present in these two powders (Section 3.2). The large crystallites would grow

rapidly at the expense of finer material during sintering, giving sintered grain sizes larger than would be predicted from Equation 4.

No theoretical justification can be offered for Equation 4. It is presented as a relationship which, for a number of sulphate-derived powders of reasonably uniform crystallite size, can predict to about ± 30 per cent. the grain size obtained for a given sintered density in the range 95-99 per cent. Electron microscopy, green density, and surface area measurements are sufficient to predict the grain size at any sintered density using this relationship. Equation 4 is not applicable after a limiting density is reached, or for powders of very non-uniform crystallite size. It remains to be seen whether Equation 4 applies to BeO powders of other derivation and purity over a wider green density range, and in the untested region from green density to 95 per cent. theoretical density.

4.4 Sinterability

Tables 3, 4, and 5 show that in general sinterability increased with increasing surface area of the powders tested. The exceptions were powders 3 and 4, which contained a high proportion of very large crystallites.

For powder compacts which vary only in the specific surface of the powder used, sintering theory (Appendix 2) predicts that a linear relationship should exist between the specific surface and the reciprocal of the sintering temperature (°K) required to achieve a given density in a given time. In the present work the powders were of similar but not identical impurity content, they differed in aggregate structure and in uniformity of crystallite size, and the pressed compacts differed in green density.

The differences in impurity content between the six powders tested would introduce some scatter about any relationship between specific surface and sintering temperature but should not obscure the overall trend.

Powders showing strong aggregation (Numbers 4, 5, and 6) might initially sinter more readily than less-aggregated material, owing to rapid shrinkage of the tightly-packed aggregates. However, this non-uniform shrinkage could lead to void formation, a slowing-down in shrinkage rate, and a limiting maximum density. Powders 5 and 6 did, in fact, show void formation and an end-point density effect (Tables 4 and 5). Thus although strong aggregation should lower the temperature required to achieve an intermediate sintered density, there should be less effect at a density close to the end-point density.

The effect of gross non-uniformity in initial crystallite size on the relationship between grain size and density has been discussed in Section 4.3. The enhanced crystallite growth process proposed there would also reduce the sintering rate of such material, the observed rate being characteristic of a surface area lower than the measured powder surface area. Powders 3 and 4, which were very non-uniform in crystallite size, probably behaved in this way. If the assumption is made that an "effective" surface area for sintering may be calculated from the observed relationship between grain size and density in each sintered material, together with the relationship between surface area and mean linear intercept (Appendix 1), the experimental results in Table 7 yield "effective" surface areas of 7.4 and 6.6 m^2/g for powders 3 and 4 respectively. As will be shown, these values give better agreement with the sintering temperatures than the respective measured powder values of 10.4 and 14.3 m^2/g.

Variations in green density are definitely important. Semi-empirical corrections can be made to the measured sintering temperature in order to normalize to a given green density; the method is described in Appendix 3.

Figure 11 shows the correlation between log (surface area) and the reciprocal of the temperature (°K) required to achieve a density of 2.90 g/cm^3 on sintering for one hour in nitrogen, normalized to a green density of 1.75 g/cm^3. This temperature was taken as a measure of sinterability because all powders exceeded or approached the density 2.90 g/cm^3 during testing and thus the temperature to achieve this density could be determined by interpolation or only minor extrapolation. In addition the conditions of one hour at temperature, nitrogen sintering, and a final density of 2.90 g/cm^3 are of technological interest at Lucas Heights.

The small circles in Figure 11 for powders 3 and 4 are points at the measured surface areas, whereas the large circles are at the calculated effective surface areas of 7.4 m^2/g and 6.6 m^2/g respectively.

Also included is a point from results previously obtained using UOX lot 200-W-216-P (Bannister 1964a).

Figure 11 shows the definite trend towards lower sintering temperature with increasing surface area. The straight line is the least-squares fit to the points given by powders 1, 2, 5, 6, and UOX lot 200-W-216-P. The points using the "effective" surface areas of powders 3 and 4 are also reasonably close to this line, the equation of which is :

$$\frac{10^4}{T} = 2.8\ (1 + \log_{10} S) \quad , \qquad \ldots\ldots\ldots\ldots\ldots\ldots (5)$$

where T °K is the sintering temperature and S m^2/g is the powder surface area.

Equation 5 refers only to compacts of green density 1.75 g/cm^3. However it may be combined with the correction term for variation in green density (Appendix 3, Equation 9, to yield the more general equation:

$$\frac{10^4}{T} = 3.4 + 2.8 \log_{10} S - 6 \log_{10} P_o \quad , \qquad \ldots\ldots\ldots\ldots\ldots\ldots (6)$$

where P_o is the actual green porosity of the material.

The standard deviation of an individual value of $10^4/T$ calculated from Equations 5 or 6 is 0.2, which in the temperature range 1200-1700 °C corresponds to a temperature deviation of 50-70 °C.

It is suggested that Equation 6 might be useful for predicting approximate sintering temperatures for sulphate-derived BeO of surface area 5 to 25 m^2/g, green density 1.5 to 1.8 g/cm^3, and low cationic impurity content.

For example, a batch of UOX powder (lot 200-W-269-P) recently received at Lucas Heights has surface area 9.7 m^2/g and a green density at 20 tons/in^2 of 1.82 g/cm^3 (J.L. Woolfrey - private communication). Substitution in Equation 6 yields T = 1750 °K or 1480 °C as the temperature required to achieve a density of 2.90 g/cm^3 on sintering for one hour in nitrogen. Analysis of results obtained on this material (T.E. Clare - private communication) suggests a "sintering temperature" of about 1460 °C, in good agreement with the predicted value.

It is stressed that Equations 5 and 6 are tentative only, and should be tested against many more BeO powders. The equations may not apply to material of other than sulphate derivation, and do not apply to powders of grossly non-uniform crystallite size. For the latter, an "effective" surface area, lower than the measured surface area, governs the sintering behaviour.

4.5 General Comments

Conclusions which may be reached on factors involved in sinterability and sintered grain size are summarised below.

1. Sinterability is enhanced by high surface area, high green density, and uniformity of crystallite size. For those powders tested which were uniform in crystallite size, Equation 6 expresses the variation of "sintering temperature" with surface area and green density, that is:

$$\frac{10^4}{T} = 3.4 + 2.8 \log_{10} S - 6 \log_{10} P_o \quad , \qquad \ldots\ldots\ldots\ldots\ldots\ldots (6)$$

2. The higher the surface area and green density, the lower is the grain size at a given sintered density. For those powders tested which were uniform in crystallite size, this effect is expressed quantitatively by the equation:

$$P^{1.25} G = \frac{1.33\ P_o^{1.25}}{S} \quad , \qquad \ldots\ldots\ldots\ldots\ldots\ldots (7)$$

which is derived from Equation 4 and the relationship between G_o and S (Appendix 1).

3. Gross non–uniformity of initial crystallite size can lead to grain sizes higher than those calculated from Equation 7.

Thus for a given material the sintering temperature may be reduced, and sintered grain sizes lowered, by increasing either (or both) the surface area or the green density. As an extreme example, which may be relevant to BeO produced by, for example, a sol–gel process, Equation 6 predicts that a powder of surface area 100 m^2/g, compacted to a green density of 1.5 g/cm^3, might be sintered in nitrogen to a density of 2.9 g/cm^3 at about 1000 °C. Equation 7 predicts that the grain size at that density might be 0.3–0.4 microns.

5. SUMMARY AND CONCLUSIONS

A study of six sulphate–derived beryllium oxide powders of similar cationic impurity contents but different surface areas has led to the following conclusions.

(a) Segregated impurities and strongly–bonded aggregates can produce non–uniform shrinkage and grain growth and even internal cracking during sintering.

(b) Sulphate–derived powders usually sintered less readily in slowly–flowing hydrogen than in nitrogen. This was possibly due to the effect of water generated by reaction between hydrogen and residual sulphate in the powders.

(c) For powders of reasonably uniform crystallite sizes, sintered densities and grain sizes tended to obey the relationship:

$$(\text{Porosity})^{1.25}\ (\text{Mean Linear Intercept}) = (\text{Green Porosity})^{1.25}\,(\text{Green Mean Linear Intercept}).$$

Green mean linear intercepts may be calculated using the equation:

$$\text{Green Mean Linear Intercept} = \frac{1.33}{\text{Surface Area of Powder}}$$

Powders with a wide spread of crystallite sizes gave higher sintered grain sizes than the values calculated from these equations.

(d) For powders of reasonably uniform crystallite size, isostatically pressed and sintered for one hour in nitrogen, the temperature required to achieve a density of 2.90 g/cm^3 decreased with increasing surface area and green density according to the equation:

$$\frac{10^4}{\text{Temperature } {}^\circ\text{K}} = 3.4 + 2.8\ (\text{Surface Area}) - 6 \log_{10} (\text{Green Porosity})$$

Powders with a wide spread of crystallite sizes required higher sintering temperatures than the temperatures calculated using this equation.

6. ACKNOWLEDGEMENTS

Some of the experimental work was performed by Mr. G.L. Wulf. The Analytical Chemistry Section performed all chemical analyses, and the Chemistry Section the surface area measurements. The electron microscopy and preparation of metallographic specimens were carried out by Materials Physics Section.

7. REFERENCES

Aitken, E.A. (1960). – Initial sintering kinetics of beryllium oxide. J. Amer. Ceram. Soc. 43: 627.

Bannister, M.J. (1964a). – Sinterability studies on various BeO powders. J. Nucl. Mat. 14: 303 – 309.

Bannister, M.J. (1964b). – The kinetics of sintering and grain growth of beryllia. J. Nucl. Mat. 14: 315 – 321.

* Coble, R.L. (1958). – Initial sintering of alumina and hematite. J. Amer. Ceram. Soc. 41: 55.

Smith, C.S., and Guttman, L. (1953). – Measurement of internal boundaries in three–dimensional structures by random sectioning. J. Metals 5: 81.

* Referred to in Appendix 2.

APPENDIX 1

THE MEAN LINEAR INTERCEPT IN A POWDER COMPACT

According to Smith and Guttman (1953) the measured mean linear intercept G in a polycrystalline body is related to the grain boundary area per unit volume S_v by the equation:

$$S_v = \frac{2}{G} \quad \ldots\ldots\ldots\ldots\ldots\ldots \quad (1)$$

In a polycrystalline body, each grain boundary surface is shared by two crystals. However in a powder each surface belongs to only one crystal. Thus in a powder Equation 1 is modified by the factor 2.

Thus $$\frac{S_v \text{ (Powder)}}{2} = \frac{2}{G} \quad \ldots\ldots\ldots\ldots \quad (2)$$

or $$S_v = \frac{4}{G} \quad \ldots\ldots\ldots\ldots \quad (5)$$

S_v is related to S, the surface area per unit mass, by Equation 6.

$$S_v = \rho S \quad \ldots\ldots\ldots\ldots \quad (6)$$

For BeO, ρ = 3.01 g/cm³. Equations 5 and 6 then yield:

$$G = \frac{1.33}{S} \quad \ldots\ldots\ldots\ldots\ldots \quad (7)$$

APPENDIX 2

THE RELATIONSHIP BETWEEN SURFACE AREA AND SINTERING TEMPERATURE

It can be predicted theoretically that in general the sinterability of powders should increase with increasing surface area. That such a relationship is not always found is probably due to over-riding variations between powders in other respects, such as impurity content, nature of aggregation, etc. However, if consideration is restricted to powders of similar physical and chemical properties, differing only in surface area, and if certain other assumptions are made, a mathematical relationship with some theoretical significance can be derived.

Coble (1958) has shown that the initial rate of densification ($-\frac{dP_o}{dt}$) of a powder compact at a temperature of T °K is related to the crystallite size r and the temperature by an equation of the form:

$$-\frac{dP_o}{dt} \propto \left(\frac{1}{r}\right)^a \quad \exp\left(-\frac{Q}{RT}\right) \quad , \quad \ldots\ldots\ldots \quad (1)$$

where a is a constant for the compact and Q is the activation energy for densification.

$$\text{Now } r \propto \frac{1}{S} \quad , \quad \ldots\ldots\ldots\ldots\ldots\ldots\ldots\ldots \quad (2)$$

where S is the surface area per unit mass.

$$\text{Therefore } -\frac{dP_o}{dt} \propto S^a \quad \exp\left(-\frac{Q}{RT}\right) \quad \ldots\ldots\ldots\ldots \quad (3)$$

It is now assumed the mechanism of densification does not vary between powders of different surface areas. This means that porosity versus time during the whole of the sintering process can be expressed as:

$$f(P) = k_{(A,B,\ldots)} \; t \quad \exp\left(-\frac{Q}{RT}\right) \quad ,$$

where f(P) and Q are the same for all powders (A,B,...) and only k varies. This is a reasonable assumption.

Thus if the powders are all pressed to the same initial density (porosity = P_o) and isothermally sintered at appropriate temperatures such that the same density (porosity = P_1) is achieved in all powders after the same sintering time t_1, then all the porosity–time curves completely coincide. If this is so then at any particular time $-\frac{dP}{dt}$ is the same for all powders and thus $\frac{dP_o}{dt}$ (at t = o) is also constant.

Equation 3 then becomes:

$$S^a \quad \exp\left(-\frac{Q}{RT_s}\right) = B, \quad \ldots\ldots\ldots\ldots\ldots\ldots \quad (4)$$

where T_s is the temperature (°K) at which a particular porosity P_1 is reached from an initial porosity P_o after a fixed time t_1 ; for chosen values of P_o , P_1, and t_1, B is a constant for all powders, while T_s can be called the "sintering temperature" of a powder.

From Equation 4:

$$a \log_{10} S \; - \frac{Q}{2.3\, RT_s} = \log_{10} B \quad \ldots\ldots\ldots\ldots \quad (5)$$

APPENDIX 2 (Continued)

A plot of $\log_{10} S$ against $1/T_s$ (for constant P_0, P_1, and t_1) should give a straight line of slope:

$$\frac{d\ (\log_{10} S)}{d\ (1/T_s)} = \frac{Q}{2.3\ a\ R} \qquad \ldots\ldots\ldots\ldots\ldots\ldots\ (6)$$

For BeO, P_1 and t_1 have been chosen as 3.7 per cent. (that is, density = 2.90 g/cm^3) and one hour respectively. T_s is therefore the appropriate sintering temperature in $^\circ$K.

APPENDIX 3

THE EFFECT OF GREEN DENSITY ON SINTERING TEMPERATURE

Sintering experiments on UOX lot 200–W–216–P of green densities 1.50g/cm^3 and 1.73g/cm^3 (Bannister, unpublished work), on UOX lot 200–W–266–P of green densities 1.64g/cm^3, 1.68g/cm^3, and 1.78g/cm^3, and on UOX lot 200–W–269–P of green densities 1.67g/cm^3, 1.73g/cm^3, and 1.82g/cm^3 (T.E. Clare – private communication), may be analysed to show that, for a given sintering temperature and time, the green porosity P_o and sintered porosity P are related by an empirical equation of the form:

$$\log_{10} P = a + b \log_{10} P_o \qquad \ldots\ldots\ldots\ldots\ldots\ldots (1)$$

Values of b from 4 to 10 have been found, but the most frequent and mean value is $b = 6$. With this value of b, Equation 1 becomes:

$$\log_{10} P = a + 6 \log_{10} P_o \qquad \ldots\ldots\ldots\ldots\ldots\ldots (2)$$

Now for UOX lot 200–W–216–P of green density 1.73g/cm^3 (Bannister 1964b) and of green density 1.50g/cm^3, and for UOX lot 200–W–266–P of green density 1.76g/cm^3 (Bannister, unpublished work), the kinetics of later-stage sintering may be described by the equation:

$$2.5 \log_{10} P + \log_{10} t = K + \frac{Q}{4.576T} \quad , \qquad \ldots\ldots\ldots\ldots\ldots (3)$$

where K depends on the green density and also varies between powders, and where the activation energy Q has a value consistently near 115 kcal/mole.

For a given powder, Equations 2 and 3 may be combined to yield:

$$2.5 \log_{10} P + \log_{10} t = A + \frac{115{,}000}{4.576T} + 15 \log_{10} P_o \quad , \quad \ldots (4)$$

where the constant A is now characteristic of the powder considered.

When P and t are given chosen values (for example, P = 3.7 per cent. for a density of 2.90g/cm^3, t = 1 hour), Equation 4 reduces to:

$$15 \log_{10} P_o + \frac{115{,}000}{4.576T} = C \quad , \qquad \ldots\ldots\ldots\ldots\ldots\ldots (5)$$

where C is a constant depending on the powder and the chosen values of P and t,

or

$$\log_{10} P_o + \frac{1680}{T} = \frac{C}{15} \qquad \ldots\ldots\ldots\ldots\ldots\ldots (6)$$

Equation 6 allows the calculation of the sintering temperature T for a standard green porosity P_o, from knowledge of the sintering temperature T' for a green porosity P_o'. Thus

$$\log_{10} \left(\frac{P_o}{P_o'} \right) = 1680 \left(\frac{1}{T'} - \frac{1}{T} \right) \qquad \ldots\ldots\ldots\ldots\ldots (7),$$

or

$$6 \log_{10} \left(\frac{P_o}{P_o'} \right) = \frac{10^4}{T'} - \frac{10^4}{T} \qquad \ldots\ldots\ldots\ldots\ldots (8)$$

and hence

$$\frac{10^4}{T} = \frac{10^4}{T'} - 6 \log_{10} \left(\frac{P_o}{P_o'} \right) \qquad \ldots\ldots\ldots\ldots\ldots (9)$$

TABLE 1

BERYLLIUM OXIDE POWDERS

Powder No.	Designation	Origin
1	UOX Lot 200–W–266–P	Brush Beryllium Co.
2	PY 60	Pechiney Co.
3	Berylco Grade V	Beryllium Corporation
4	CH–grade	NGK Insulators (Japan)
5	CF–grade (Sample 1)	NGK Insulators
6	CF–grade (Sample 2)	NGK Insulators

TABLE 2

ANALYSIS OF BeO POWDERS (A.A.E.C.)

Impurity p.p.m. (BeO basis)	Powder 1	Powder 2	Powder 3	Powder 4	Powder 5	Powder 6
Na	<35	<35	<35	<35	~35	<35
Mg	60	10	10	20	<10	50
Ca	<20	<20	35	<20	25	100
Al	35	80	15	50	75	30
Si	50	25	40	50	45	100
Fe	25	25	15	<20	15	50
Zn	<35	<35	<35	<35	<35	<35
Ni	<20	<20	<20	<20	<20	<20
Cr	<20	<20	<20	<20	<20	<20
C	310	340	650	400	Not determined	1160
F	<5	<5	12	8	Not determined	16
S	740	1470	870	230	Not determined	2000

TABLE 3

PHYSICAL PROPERTIES OF BeO POWDERS

Powder No.	Surface Area (m^2/g)	Mean Crystallite Diameter (microns)	Mean Linear Intercept (microns)	Pour Density (g/cm^3) ± 0.01	Tap Density (g/cm^3) ± 0.02	Green Density at 20 tons/in^2 (g/cm^3) ± 0.02
1	9.5	0.21	0.140	0.34	0.45	1.76
2	8.1	0.25	0.165	Not determined	Not determined	1.69
3	10.4	0.19	0.128	0.27	0.39	1.68
4	14.3	0.14	0.093	0.64	0.84	1.65
5	20.4	0.098	0.065	0.89	1.11	1.66
6	24.1	0.083	0.055	0.77	0.99	1.62

TABLE 4

DENSITIES AFTER SINTERING 1 HOUR IN N_2
(120 p.p.m. water vapour)

Powder No.	Sintered Density (g/cm^3)						
	1210 °C	1250 °C	1300 °C	1400 °C	1500 °C	1600 °C	1700 °C
1	–	–	–	–	2.85	2.93	2.95
2	–	–	–	–	2.83	2.92	2.93
3	–	–	–	–	2.69	2.79	2.89
4	–	–	–	–	2.71	2.83	2.93
5	–	–	2.87	2.93	2.93	2.93	2.94
6	2.56	2.80	2.93	2.97	2.97	–	–

TABLE 5

DENSITIES AFTER SINTERING 1 HOUR IN H_2

(60 p.p.m. water vapour)

Powder No.	Sintered Density (g/cm^3)				
	1300 °C	1400 °C	1500 °C	1600 °C	1700 °C
1	–	–	2.83	2.93	2.95
2	–	–	2.79	2.89	2.95
3	–	–	2.64	2.75	2.85
4	–	–	2.67	2.73	2.93
5	–	–	2.83	2.83	–
6	2.85	2.95	2.96	–	–

TABLE 6

GRAIN SIZES (MEAN LINEAR INTERCEPTS) AFTER SINTERING 1 HOUR

Powder No.	Grain Size (microns)									
	1300 °C		1400 °C		1500 °C		1600 °C		1700 °C	
	N_2	H_2	N_2	H_2	N_2	H_2	N_2	H_2	N_2	H_2
1	–	–	–	–	1–2	–	2.5	4.9	5.5	9.9
2	–	–	–	–	–	–	3.9	3.1	4.9	5.7
3	–	–	–	–	–	–	1.9	–	3.5	2.6
4	–	–	–	–	–	–	2.3	–	7.5	5.1
5	~1	–	2.1	–	5.4	3.5	7.8	3.7	11.4	–
6	~1	<1	3.8	2.3	10.1	8.0	–	–	–	–

TABLE 7

THE RELATIONSHIP BETWEEN GRAIN SIZE AND DENSITY

(All specimens sintered 1 hour at temperature)

Powder No.	$(P_o^{1.25} G_o)$	$(\text{Porosity})^{1.25}$ (Mean Linear Intercept)									
		1300 °C		1400 °C		1500 °C		1600 °C		1700 °C	
		N_2	H_2	N_2	H_2	N_2	H_2	N_2	H_2	N_2	H_2
1	15	–	–	–	–	8–16	–	9	17	13	24
2	19	–	–	–	–	–	–	15	18	17	13
3	15	–	–	–	–	–	–	23	–	20	21
4	11	–	–	–	–	–	–	22	–	26	18
5	7.6	~7	–	7	–	19	33	27	35	34	–
6	6.7	~4	<8	5	5	14	15	–	–	–	–

(X 30,000)

FIGURE 1. POWDER 1

(X 30,000)

FIGURE 2. POWDER 2

(X 15,000)

FIGURE 3. POWDER 3

(X 15,000)

FIGURE 4. POWDER 4

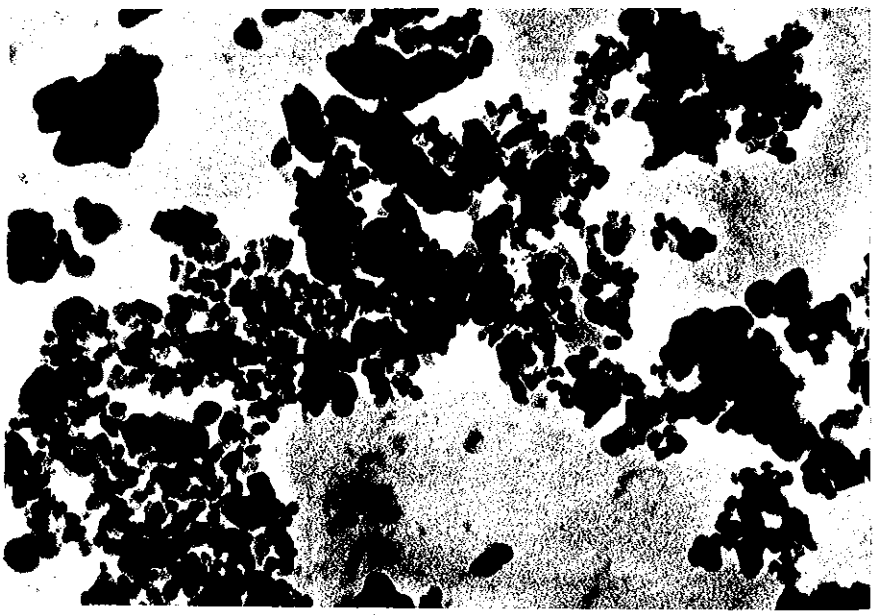

(X 30,000)

FIGURE 5. POWDER 5

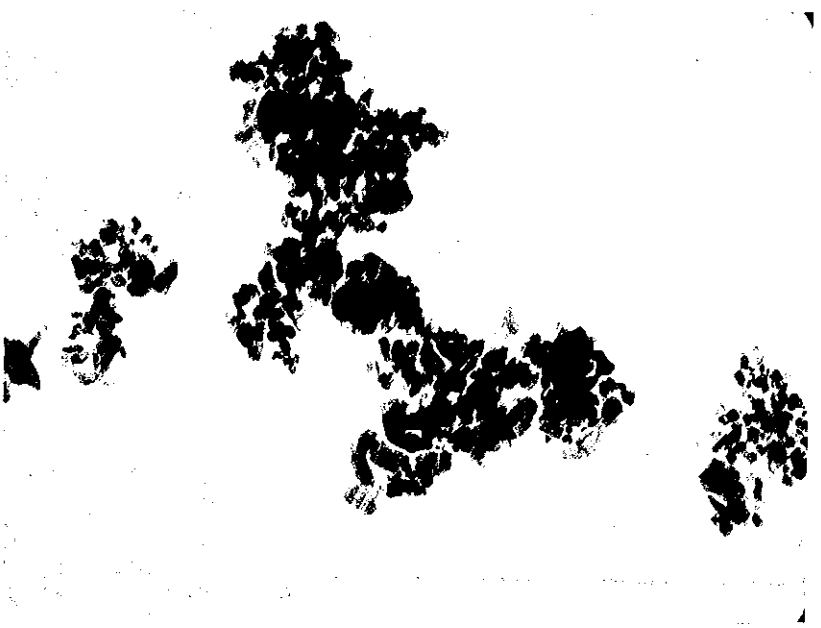

(X 30,000)

FIGURE 6. POWDER 6

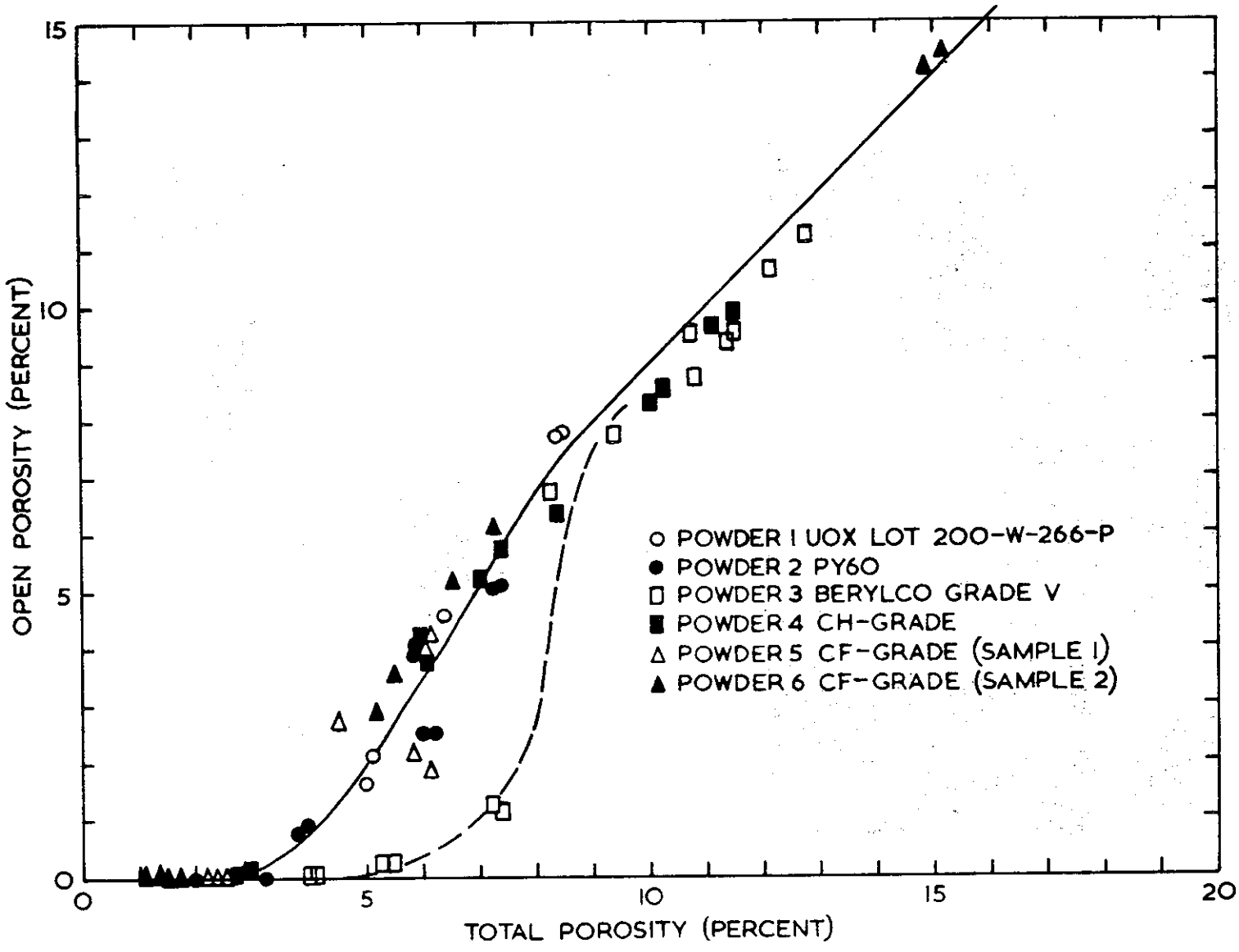

FIGURE 7 OPEN POROSITY VERSUS TOTAL POROSITY FOR SINTERED COMPACTS

P782

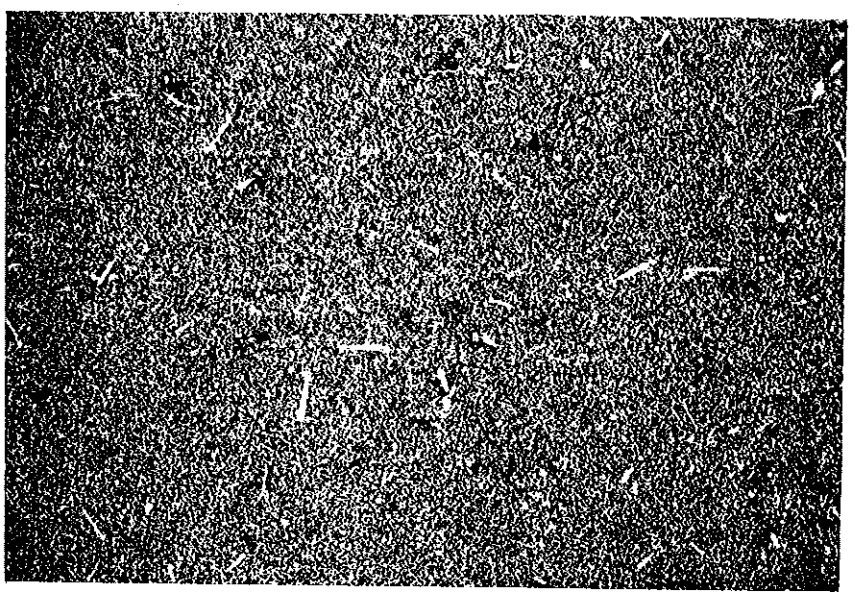

(X75)

FIGURE 8. NEEDLES IN POWDER 1. SPECIMEN SINTERED 1 HOUR AT 1500 °C IN N_2. DENSITY 2.86 g/cm³

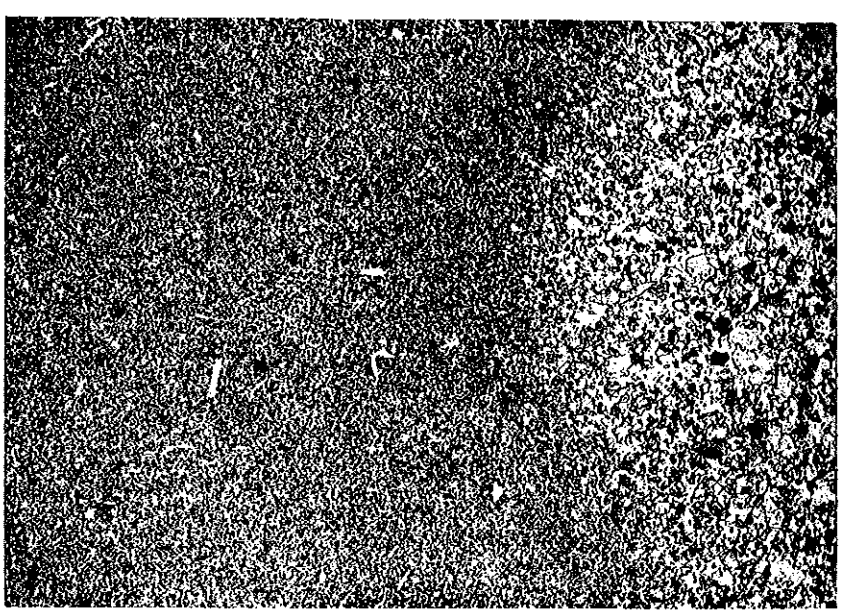

(X75)

FIGURE 9. A COARSE-GRAINED AREA IN POWDER 1. SPECIMEN SINTERED 1 HOUR AT 1500 °C IN N_2. DENSITY 2.86 g/cm³

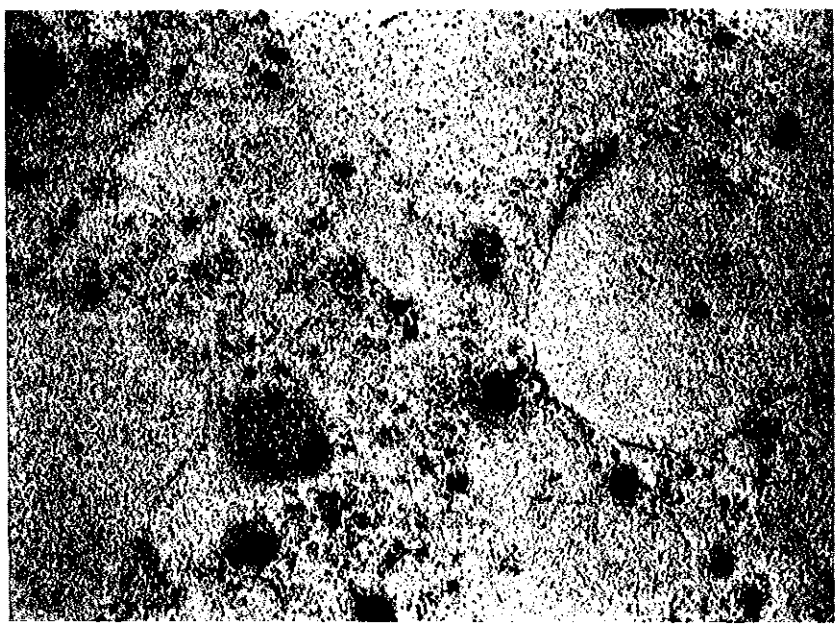

(X 100)

FIGURE 10. INTERNAL CRACKING IN POWDER 6. SPECIMEN SINTERED 1 HOUR AT 1300 °C IN N_2. DENSITY 2.93 g/cm^3

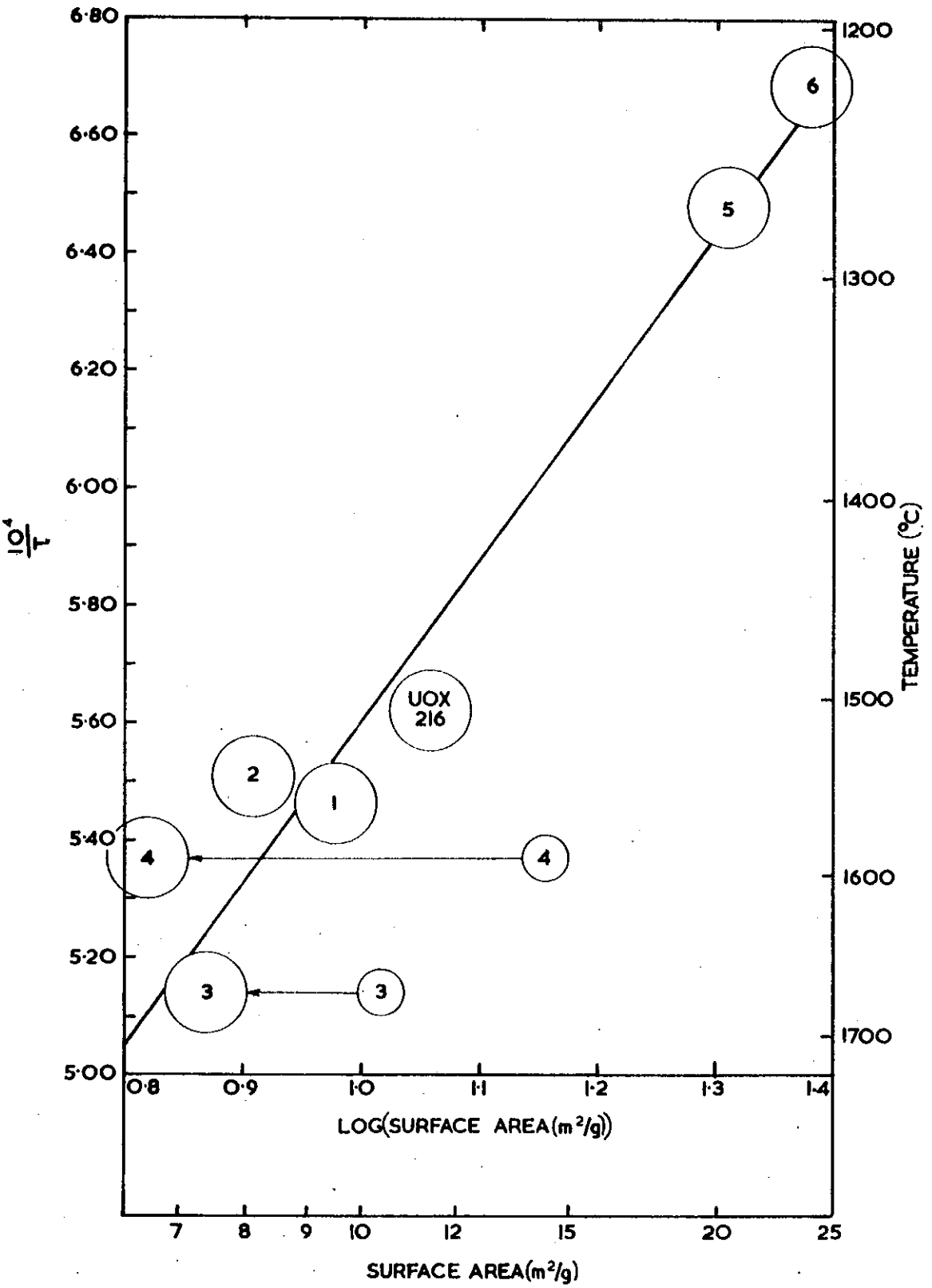

FIGURE II RELATIONSHIP BETWEEN "SINTERING TEMPERATURE" AND SURFACE AREA

P782